Primary Loop Study of a VVER-1000 Reactor
With special Focus on Coolant Mixing

Michael Böttcher

Institut für Reaktorsicherheit (IRS), Forschungszentrum Karlsruhe GmbH- KIT

Abstract

In this paper a detailed model of a VVER1000 reactor pressure vessel (RPV) with the extension of simplified primary loops is presented (Loop model). The primary loop components like steam generators and pumps are modelled by the outer shapes and additional source terms for energy and momentum exchange. The RPV model part is tested without primary loops and compared with former results obtained with a coarser model. The intention of this work is to demonstrate the abilities of modern CFD tools like ANSYS CFX to model technical facilities with complex geometry such as a reactor pressure vessel with its primary loops over all relevant scales from a range of approximately 1mm up to a largest dimension of around 50m. As an example, the rotation of flow patterns at the core inlet derived from plant data obtained at the Kozloduy Nuclear Power Plant (Unit 6) is simulated. As progress against the RPV model the Loop model is able to predict a swirl of flow patterns but due to the lack of technical details like the pump impellers the swirl is overestimated.

1. Introduction

At the Institute of Reactor Safety (IRS) of the Forschungszentrum Karlsruhe the application of CFD methods for nuclear reactors started in context with the Coolant Transient Benchmark of a VVER-1000 pressurized reactor from power plant station at Kozloduy, Bulgaria (Unit 6) initiated by OECD in 2002. In 2006 a detailed CFX model with some geometrical simplifications containing all relevant parts of the pressure vessel was presented [1] at CFD4NRS in Munich. One essential deficiency of this model was the incorrect prediction of the observed swirl of flow patterns at the core inlet.

It was assumed that the reason for the swirl effect could be found inside the primary loops. Therefore the previous model of the pressure vessel was improved by some more geometrical details, partially a better spatial resolution and a simplified consideration of the primary loops.

The model presented in this paper is based on the pre-mentioned work. In the former work better agreement with experimental data was obtained by using a first order donor-cell method for the spatial discretization. The influence of missing geometrical details in the lower plenum was compensated by numerical diffusion of the 1st order method. As consequence additional geometrical details in the lower plenum are now taken into account. Furthermore the grid spacing in the downcomer and the lower plenum is refined now. The results from the improved RPV model show less sensitivity on the discretization scheme and recalculated transient hot leg temperatures transients are improved now.

The testing and development procedure is divided into two parts. The first one considers the RPV with all its details while the second one includes all parts of the model with the extension of the primary loops and its components. For this model named RPV model the flow is controlled by boundary conditions at the cold leg inlets and hot leg outlets. The broader model which includes the primary loops – named Loop model - does not contain any inlet and outlet conditions because a closed system is considered. In this case the flow is controlled by momentum and energy source terms which have to be specified for the pumps and steam generators. The source terms have to be adjusted to measured flow conditions (flow rates and temperatures) which make the numerical control of the flow more difficult.

A crucial point is the large spread of scales over several orders of magnitudes. The overall height of the pressure vessel is 12.5m and its inner diameter amounts to 3.6m. The outer dimensions of the primary loops are approximately 40m x 20m x 20m while the smallest components inside the RPV that influence the coolant mixing are in the range of 1mm. It becomes clear that the layout of the computa-

tional grid due to scale resolution, the computer memory limit and reasonable computational time is of highest priority for successful simulations. Together with the just mentioned first version the construction of the grid and testing of the model took about 2 years especially for the later on presented Loop model.

The number of cells has increased by more than a factor of 2 against the basic model from 2006. The former RPV model consisted of 14.5 million cells while the new models are created with approximately 24 and 34 million cells. The parental model was constructed by three blocks forming the downcomer with the lower plenum, the core and the upper plenum with non-matching cells at the boundary layers. The blocks were fitted together by two GGI (General Grid Interface) layers which increased the computational time up to 20% for one layer. In a first attempt the Loop model was constructed in the same way which resulted in 2 additional interfaces per primary loop so that the model included 10 GGI layers. As consequence a steady state analysis as parallel application with 12 processes took around 1 month of CPU time so it was not possible to run a number of parameter studies in a reasonable time. A basic problem was given by the PC´s management system (WINDOWS XP 32 bit) which is only able to handle processes up to a memory size of around 1.5 GB independent on the total memory available which resulted in a maximum grid size of 10 million cells for a single block. This was resolved by switching to a 64 bit system which allows the generation of large grids as single blocks without GGI interfaces.

The simulations were performed on a 64 bit Linux cluster with 12 processors. By elimination of the interfaces the computational time for the RPV model could be reduced from 1 month to about 2 days. For the loop model up to 1 week for a steady state simulation and approximately 4 weeks for a transient case were used. The reason for the disproportionate increase can be found in the worsened convergence behaviour.

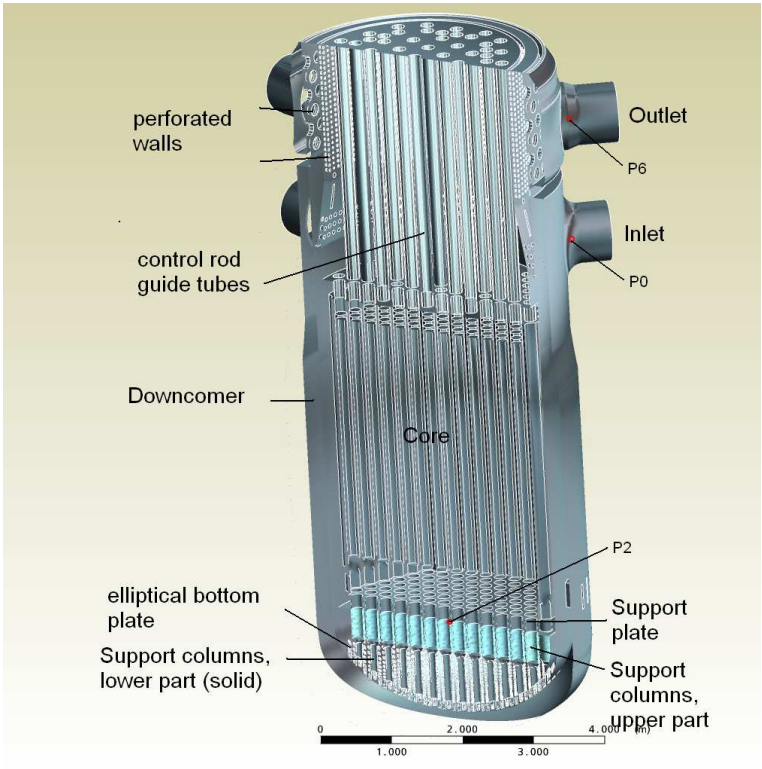

Fig. 1: The RPV model

2. Model description

Fig. 1 shows a cut through the RPV model. The average length scales of the cells especially in the downcomer are reduced now by a factor of 2 to 50mm. In the lower plenum details with significant influence on coolant mixing are included additionally like an elliptical, perforated bottom plate and core support columns with full detail resolution of its lower parts and a detailed representation of the perforated upper parts by pressure loss coefficients. As mentioned before the nodes at the block boundaries are matching now so that GGI interfaces are eliminated. Fig. 2 presents a part of the mesh from the lower plenum. The number of cells for this model part has increased from 2.6 millions to 13.4 millions. The RPV model consists of 23.8 million cells, by which 9.6 million are used for the mesh of the upper plenum containing char-

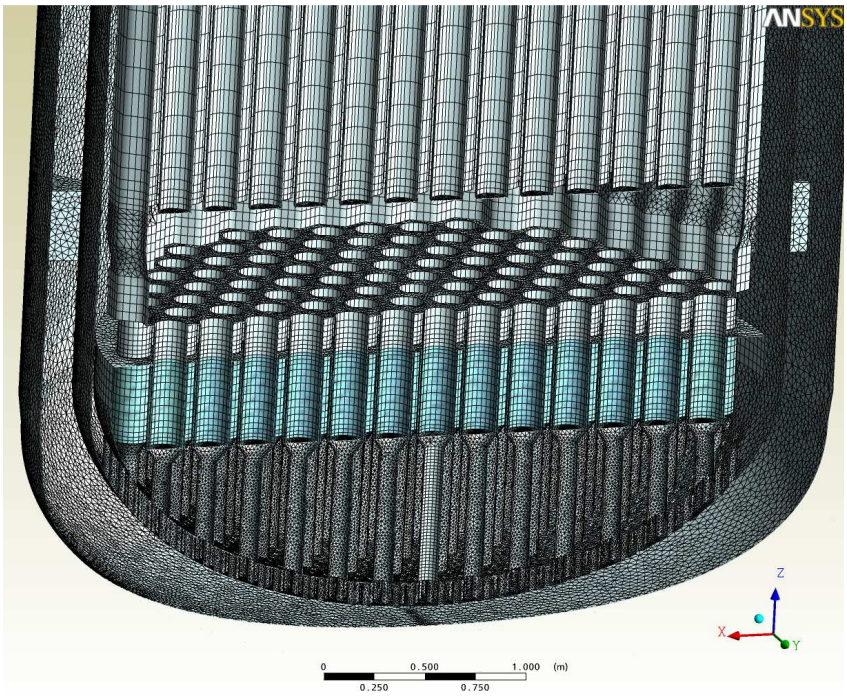

Fig. 2: Mesh from the lower part of the RPV

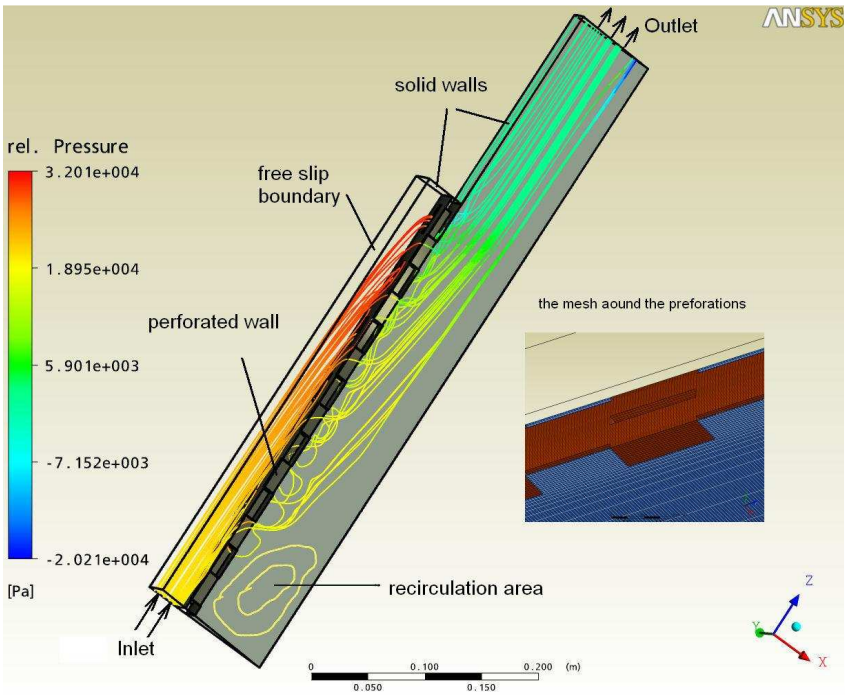

Fig. 3: Detailed model from the perforated part of a standard support column

acteristic elements like the outlet nozzles, two perforated walls and control rod guide tubes. The hexahedral core is constructed by 0.8 million structured cells representing 163 individual assemblies. Each assembly is formed by a hexahedral channel with a circular empty core, so that a blocking of 46% is achieved and individual pins are not considered. The primary loops are meshed with approximately 10 million cells so that the Loop model contains 34 million cells. For the inlet nozzles, the downcomer and some parts of the lower plenum a CAD model by Bieder [2] was used. For other parts like the elliptical bottom plate or the upper plenum the construction was performed directly from technical drawings provided within the VVER-1000 coolant transient benchmark [3].

In comparison to the parental version of the mesh, the inlets, downcomer and lower plenum are meshed completely new with finer spatial resolution and some more details such as an elliptical bottom plate perforated by 1344 holes with a diameter of 40mm and the perforated upper part of the core support columns. In locations inside and around such holes the average grid spacing is reduced to 10mm. In the former version the elliptical bottom plate was modelled as a free volume with a spatially homogeneous loss coefficient. The holes are now (coarsely) resolved by the grid so that no additional loss coefficient is necessary anymore. For the upper part of the support columns it was not possible to resolve all geometrical details.

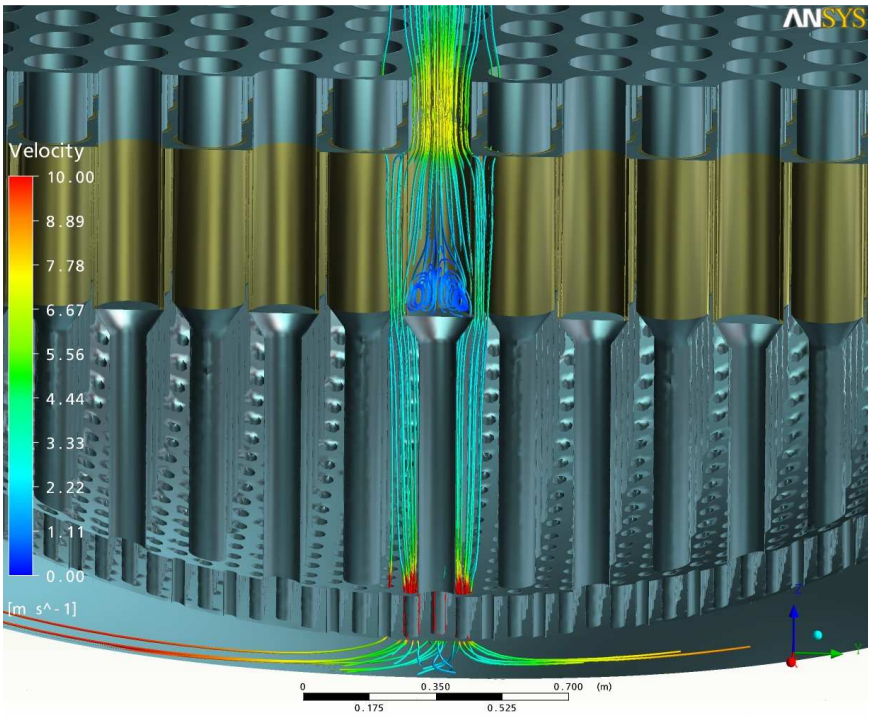

Fig. 4: The flow around a standard support column at the lower plenum

Each of the 163 support columns is formed by a solid cylindrical lower part and a tube like upper part perforated by 14 rows with together 420 slots and at the 42 peripheral positions by 12 rows with 360 slots. The length of each slot is 30mm at a width of 3mm and a wall thickness of 12 mm. For the two type of columns detailed models consisting of around 250000 cells for the evaluation of the pressure losses were developed, see Fig. 3. The detailed model resolves a 12° part in full detail. The spatial boundary resolution was chosen that y^+ at the perforations is in a range around 10. For the characteristic coolant flux of 17.9 tons/s water through the whole system, 540 K and a system pressure of 15.6 MPa pressure losses of around 24000 Pa for a column at a peripheral position and 22000 Pa for a standard position tube between the inlets and the outlets of the tubes were calculated. In the resulting reactor models these perforations and the free inner parts are considered as free flow volumes with additional pressure loss coefficients for the perforated wall parts dependent on the position of the column. The loss coefficients were adjusted by the calculated pressure losses from these perforations.

The benchmark specifications provide some pressure data for steady state conditions which are used in order to control the model accuracy especially for the new model parts. Between the inlet and a location just below the core support plate the design pressure drop P0-P2 (see Fig. 1) for nominal steady state conditions (17.9 tons/s coolant flux) is specified as 0.1971 MPa while the new RPV model predicts 0.170 MPa without any adjustments. The overall pressure drop P6-P0 is specified as 0.376 MPa and calculated as 0.359 MPa which means that the pressure losses are underestimated (up to 15% locally) by the model.

It was also tried to model the perforations with a porous media approach but this would have required a much better spatial resolution in radial direction as if prospected. Within the RPV and Loops model the perforated upper part of each support column is resolved by approximately 6000 cells. The flow structures are fitting quite well, if the streamline plots from the detailed model by Fig. 3 are compared with those of the full model presented by Fig. 4. In radial direction the perforated walls are represented only by one cell which leads in case of a porous media approach to convergence difficulties. The location marked by ‘perforated wall´ was affected by an additional isotropic pressure loss term.

The implementation within CFX [4] is done by the momentum equation:

$$\frac{\partial(\rho U_i)}{\partial t} + \frac{\partial(U_j U_i)}{\partial x_j} = -\frac{\partial p}{\partial x_i} + \rho g_i + \frac{\partial \tau_{ij}}{\partial x_j} + S_i^M \quad (1),$$

where S_i^M is a source term defined by

$$S_i^M = -C_1^R U_i - C_2^R \,|U|\, U_i + S_i^{spec} \quad (2).$$

C_1^R and C_2^R are linear and quadratic resistance coefficients. S_i^{spec} is a user defined additional source. For the quadratic resistance coefficient a value of 180 [kg/m^4] for the perforations of the standard columns and 220 [kg/m^4] for those at the peripheral, outer positions is used.

For the core model which resolves the assemblies but does not take the individual fuel pins into account additional pressure loss coefficients defined by

$$-\frac{\partial p}{\partial x} = \lambda \frac{\rho}{2} |u| u \quad (3),$$

where u is the velocity component in streamwise direction and ρ is the density of the fluid, are introduced. For the assemblies λ=3 is assumed. The core is surrounded by a bypass channel which carries app. 3% of the total mass flux. For the bypass channel λ=1.2 is used. These values were obtained by captured measured pressure losses.

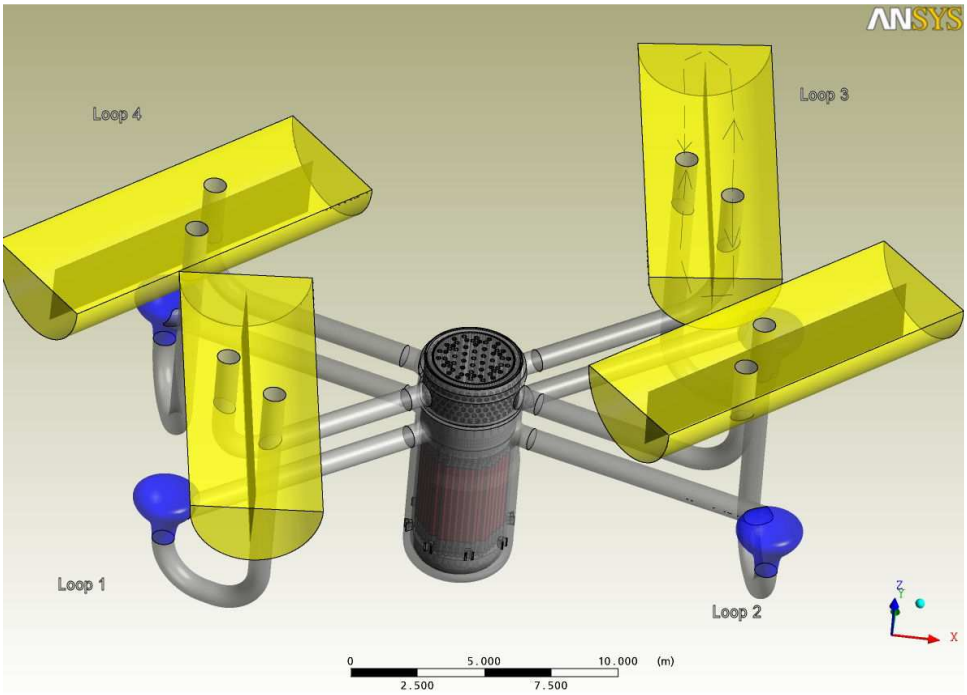

Fig. 5: The Primary Loop model

The latest model within this series is the extension of the new RPV model with the primary loops and its components like the steam generators and pumps, see Fig. 5. One essential problem for this most ambitious project was the lack of technical specifications being available. It was not possible to get CAD data or even a less detailed geometrical description about the impeller shapes of the pumps. The results show that a recirculation zone at the outlet of the pumps and the rotation of the impellers have a strong influence on the coolant mixing process until the flow enters into the lower plenum of the RPV. As consequence the interaction of the impellers with the fluid has to be modelled by volumetric momentum source terms derived by measured mass flow rates. Within the pump housing a constant axial pressure gradient was introduced adjusted by the measured mass flows rates of each loop. The implementation follows (1) and (2) by using a value of S_i^{spec} =1.30*10^6 [kg m^{-2} s^{-2}] for the axial component in a local cylindrical coordinate system. In fact the interaction of the impellers with the coolant is a 3D, instationary process. When passing through the pump the fluid suffers a pressure increase between inlet and outlet, additionally a radial and circumferential local instationary momentum transfer through the interaction with the impellers. Finally the impellers are acting as turbulence source. For a detailed quantitative analysis an implementation of the impeller shapes together with a frozen rotor approach or a sliding mesh implementation for consideration of their rotation is necessary.

The four cylindrical steam generators are forming a pool which is crossed by around 11000 u-pipes containing the primary fluid. In the model the secondary side is not considered and the u-pipe structures are not resolved in detail and are covered only by a porous media approach in order to get the correct mean flow residence times and pressure losses.

Furthermore the heat transfer through the u-pipe walls is introduced as a constant volumetric heat source based on plant data and with linear dependency on the difference between the mean fluid temperature at the entrance of the steam generators and a constant temperature on the secondary side. In Fig. 5 the flow path within the steam generator of loop 3 is indicated. After the entrance into the steam generator the flow separates into 2 parts with approximately the same fluxes and moves along an internal wall towards the outlet. The total amount of heat removal $Q_{j,tot}$ from steam generator j is calculated as

$$Q_{j,tot} = -Q_0 \frac{\overline{T}_{j,p} - T_{j,s}}{T_{j,p0} - T_{j,s}} \quad (4),$$

where Q_0 is a given total amount of heat at a reference point, $T_{j,s}$ is the temperature from the steam generators primary side at a reference point, $T_{j,p0}$ is the temperature at the entrance of the steam at reference conditions and $\overline{T}_{j,p}$ is the volume-averaged temperature from the RPV outlet until the inlet of the steam generator. This equation implies that the mass flux and pressure at the secondary side are equal or very close to those at the reference point. Moreover the heat transfer is direct proportional to the temperature difference between the primary and secondary side. It has to be mentioned that it is not sufficient to define a heat source independent on the fluid temperature because the loop model is a closed system without inlets or outlets where the fluid temperature can be specified. As the nuclear sources of the core are specified as absolute values and the outer walls of the system are considered as adiabatic, eq. (4) is the only possibility for the solver to adjust the temperature of the fluid.

The nuclear heat sources of the pins are introduced as a volumetric source dependent on the individual assembly and its local axial position. For all presented cases the heat sources are derived from a PARCS simulation described by Sanchez and Böttcher [5].

For the Loop and the RPV model a SST (Shear Stress Transport) turbulence model is applied. It has to be mentioned that in the previous RPV model version which is referenced in chapter 4 for comparison of results a standard k-ε model was used. For the spatial discretization a 1st order donor cell and the standard 2nd order method by CFX is used in order to check influences on the results. The time integration was performed by using a 2nd order Euler-Backward method.

3. Description of the scenario – boundary conditions

During the plant-commissioning phase of the Kozloduy nuclear power plant a well documented series of experiments for studying the mixing process of the loop flows in the pressure vessel were performed [6]. The reactor power is at a level of 9.6% of its thermal reference power of 3000MW so that the feedback between thermal hydraulics and the neutronics is weak and the process can be considered as a thermo-hydraulic problem. Starting from a steady state situation where all pumps are providing nearly the same flow rate of approximately 4600-4700 kg/s at a core power of 281 MW loop 1 gets isolated from its steam generator. During the next 20 minutes a heat up of 12 K is observed. Another 10 min later a new steady state situation is reached. Within the transients the core power increases to 286 MW.

The following conditions and model parameters are used for the initial steady state calculations for the different model versions:

Table 1: Boundary conditions for the RPV model

Loop no	Inlet temperatures [K]	Flow rate [kg/s]	Rel. outlet press. [Pa]
1	541.72	4737	0
2	541.65	4718	0
3	541.88	4682	0
4	541.85	4834	0

For the transient simulations the flow rate and inlet boundary conditions for the RPV model are presented by Fig. 6.

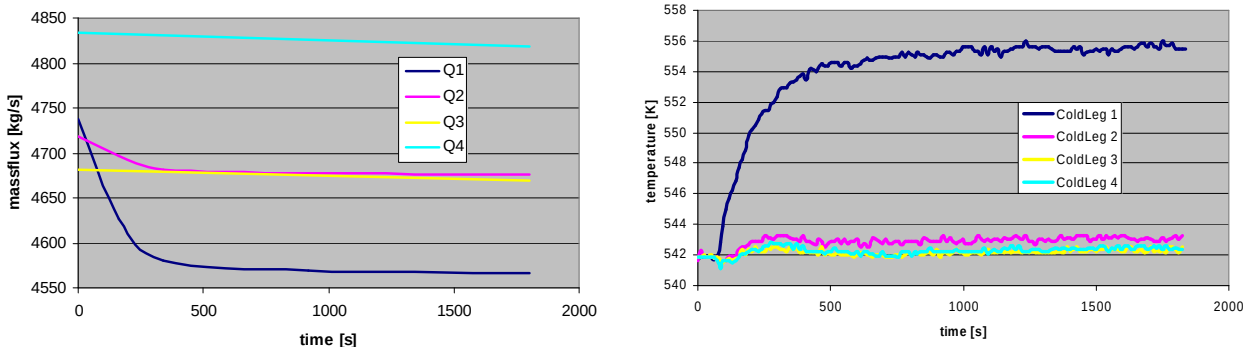

a) Flow rates at the inlets b) Inlet temperatures

Fig. 6: Transient boundary conditions for the RPV model

In case of the Loop model the system is closed so that no boundary conditions can be specified. The mass fluxes are controlled by the momentum source terms of the pumps while the fluid temperature are handled by the heat source terms of the steam generators. The precision by which the max fluxes and fluid temperatures can be established is much lower due to numerical fluctuations from the solution which would require a longer integration time. The accuracy of the flow rate plant data was specified by ±2.2%. The steady state simulations for the loop model were accepted as solution if the mass fluxes were moving within the just mentioned error range around the measured data. Furthermore for all cases presented in this paper the simulation was considered to be converged if all normalized residuals were below 5e-04 and the global balances especially for energy were fulfilled with an accuracy less than 1%.

For the steady state calculations it is assumed that all steam generators remove the same amount of heat because the flow rates in the loops and the heat transfer conditions in the steam generators are nearly equivalent. Some additional information is introduced by the specification of the heat removal term. For calculation of the source terms given by eq. (4) the parameters are given by Table 2.

Table 2: Parameters for calculation the heat removal by the steam generators by eq. (4)

	Loop 1	Loop 2	Loop 3	Loop 4
$T_{j,s}$ [K]	541.72	541.65	541.88	541.85
$T_{j,p0}$ [K]	545.0	544.78	545.03	545.0

Q_0 is assumed to be 70.25MW. It has to be mentioned that $T_{j,p0}$ are the measured temperatures at the RPV outlets.

For both models the system pressure is assumed to be 15.6 MPa. All outer model boundaries are considered as adiabatic. Furthermore no solids are considered. In case of transient calculations with the Loop model the parameters given by Table 2. Q_0 and the momentum source terms from the pumps are left constant. For loop 1 Q_0 is set to 0 MW for initiating the heat up.

4. Selected model results

For comparison, several plant data such as thermocouple measurements at the main inlets and outlets, from the assemblies at the core outlet and flow rates are available, see [3]. Additionally mixing coefficients derived from thermocouple measurements are used. The accuracy of temperature measurements is specified by ±2K. The error for mixing coefficients is not specified. At first a steady state analysis

of the temperature distribution at the core outlet is presented. The theoretical average temperature rise can be very easily calculated as approximately 3.3K by using a flow rate of 0.97*17900 kg/s, a thermal heat release of 281 MW and a specific heat capacity from the coolant (water) of 4900 J/kg K. The figures 7 and 8 show a comparison of the assembly outlet temperatures for the RPV model and the Loop model. The core consists of 163 assemblies. Their numbering is visible in figure 10.

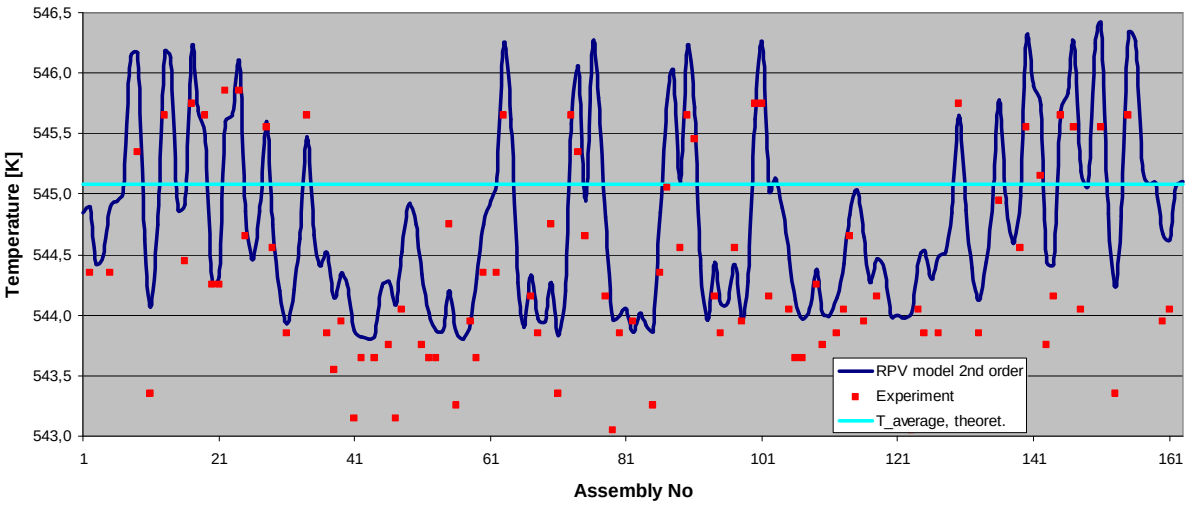

Fig. 7: Assembly outlet temperatures for the RPV model

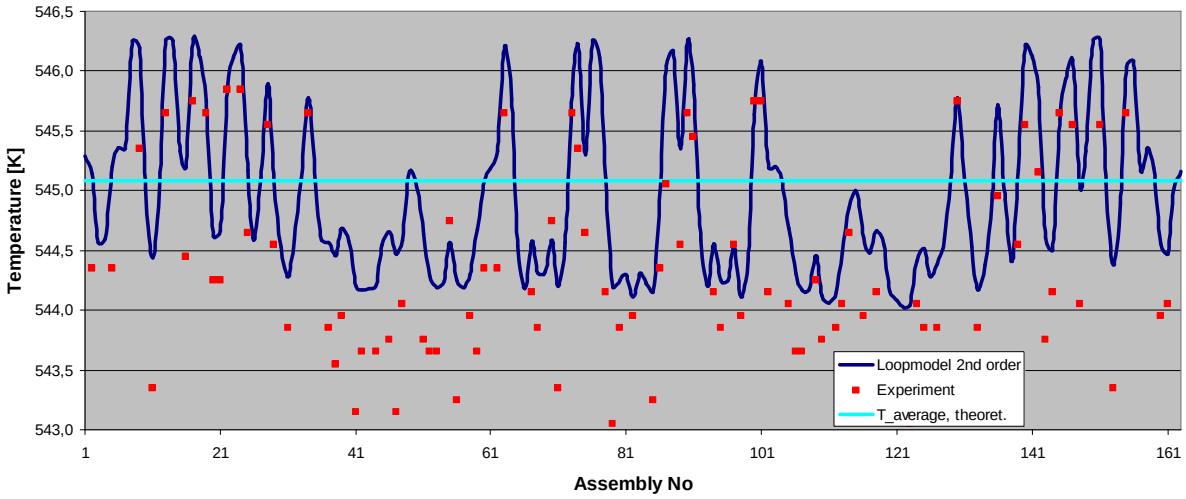

Fig. 8: Assembly outlet temperatures for the Loop model

The predicted temperatures from both models are quite similar which means that the velocity distribution at the core inlet is more or less invariant against different conditions of velocity and turbulence parameters at the inlets of the downcomer if the total mass fluxes are the same. Also the temperatures at the RPV inlets are quite similar, see Table 1. The differences between simulations and measurements are less than 1.2 K, i.e. within the accuracy of the thermocouple measurements. The measurements are about 0.5K below the theoretical core outlet temperature of 545.08K, while the predicted averaged assembly outlet temperature are 544.77K (RPV model) and 544.95K (Loop model).
These are good results because the increase of the internal energy at the core region is low against the total internal energy. The global energy balance of the simulations was fulfilled with an accuracy of 1‰ which reveals excellent convergence behaviour.

In Fig. 9 the steady state temperature distribution from the Loop model together with the flow situation at loop 1 illustrated by streamlines is shown. The temperature distribution within the core shows hot spot regions which is a consequence of fuel assemblies with higher enrichment. The coolant flows into the downcomer with a temperature around 542 K. By passing through the core it is heated up by 3.3K in average. On its way to the RPV outlets through the upper plenum with guide tube structures two perforated walls have to be passed. When leaving the vessel the temperature gradients have decreased but temperature stratifications are still visible in the pipe connections to the steam generators.

An effect which could not be reproduced by any model was the anti-clockwise rotation of flow patterns at the entrance of the core. The loops from unit 6 of the Kozloduy power plant are asymmetric placed in circumferential direction against the core. The displacements are only in a range of 3° so that they cannot explain the flow pattern rotations in the observations.

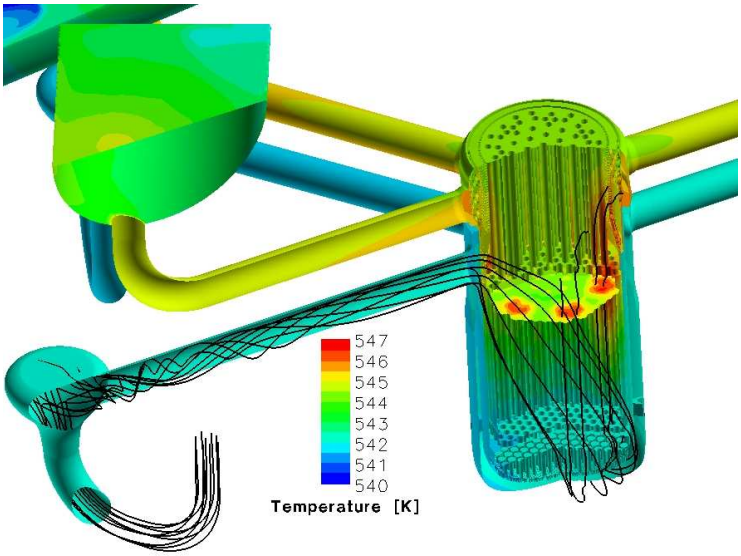

Fig. 9: Steady state temperature distribution from the RPV model

Figs. 10, 11 and 12 are presenting a comparison of mixing coefficients from loop 1 from the RPV and Loop model with plant data taken from [3]. Mixing coefficients can be understood as mass fractions within a control volume which originates from the loop concerned. From measurements can be seen that loop 1 influences a segment with an angle of approximately 120°. The central area of influence with mixing coefficients close to 1 (red colour) shows an anti-clockwise rotation of around 15°. The new RPV model predicts a distribution with an angular spread of 105° and nearly no rotation of the central area.

The Loop model predicts a rotation from the center of about 90° which is much stronger then observed in the experiments. The area of influence spreads about more than half of the total cross section. The situation is demonstrated by a streamline plot in Fig. 9.

The reason can be found in the pump model. At the asymmetric placed outlet an axial circulation is formed. Because of the boundary friction at the pipe walls on the way to the vessel inlet the circumferential velocity component decays but at the entrance of the vessel a significant part still exists. The flow swirl seems to be significantly overpredicted.

The final part of results which is presented considers the transient heat-up from loop 1. Figs. 13-16 are presenting a comparison of temperature measurements for the heat-up scenario taken at the outlets from the pressure vessel against model results from the old and new RPV model. For all transients a time step of 12s is used. Both models predict the temperature rise of the disturbed loop quite well but the new RPV model shows an overprediction of about 2K. This refers to an underestimation of the mixing process between the disturbed loop and its neighbours due to other influences not taken into account. The time delay observed in the experimental data is reproduced now much better by the new model. Furthermore the time fluctuations of the measurements can be found in the simulations, see Fig. 14 and 15. Even the fluctuations with a lower frequency can be in principle reproduced now by the new model.

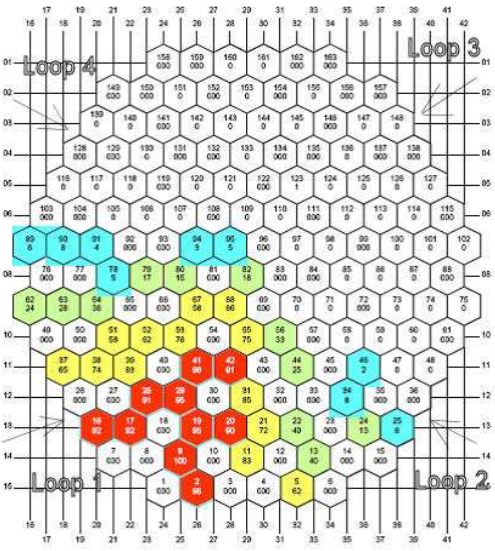

Fig. 10: Mixing coefficients – Loop 1 Plant data

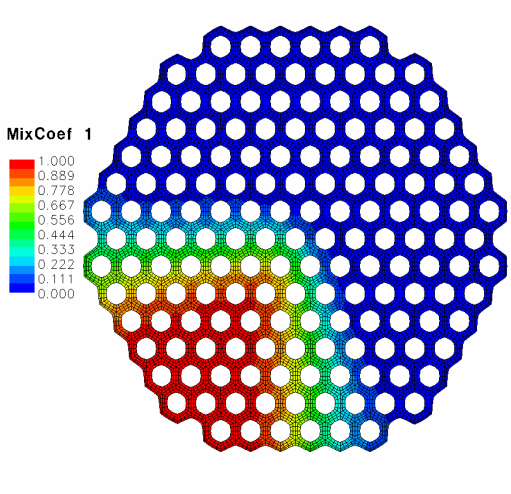

Fig. 11: Mixing coefficients – Loop 1 RPV model

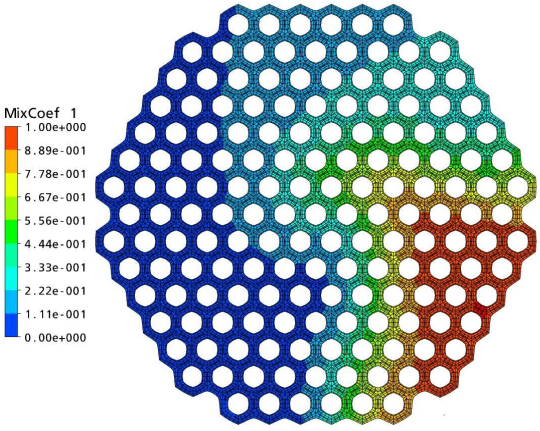

Fig. 12: Mixing coefficients – Loop 1 Loop model

One exception seems to be given by loop 4 (Fig. 16), where the older results are much closer to the observations. The interaction with the disturbed loop is strongly overpredicted by the new RPV model using a 2nd order method.

As can be seen in the predictions, there is an influence of the discretization method especially for the transient cases. The most significant influence is found at loop 4 which is located on the left hand side at the immediate neighbourhood of the disturbed loop 1 while at the other loops the influence of the discretization scheme is much smaller. Surprisingly the 1st order method is much closer to the measured data. In a previous model version with a coarser grid this behaviour was found for all loops and could be explained by the compensation of missing turbulent mixing by the increased numerical diffusion of a 1st order method. The reason is not clear and needs further investigations. Additional tests with different turbulence models and with shorter time steps have lead to very similar results.

First transient simulations with the Loop model (see the red curves in Fig. 13-16) show that the heat-up from loop 1 is significantly underestimated. Due to the much stronger swirl in the downcomer the temperature rise at loop 2 is significantly above the measurements. The heat up of Loop 4 is underestimated. This can be understood as consequence of the overestimated anti-clockwise swirl which separates the interaction areas from loop 1 and 4. Without implementation of the pump impellers or (and) additional artificial tasks like damping of the flow swirl at the cold legs between the pumps and the RPV inlets an accurate reproduction of the plant behaviour seems to be not possible.

5. Summary and outlook

Based on a former work a CFX model for the RPV of a Russian VVER1000 pressurized reactor with increased spatial grid resolution including all relevant geometrical details is presented. The model is extended by simplified primary loop components like pipes, pumps and steam generators. Due to the complexity and the lack of geometrical detail information the pumps and steam generators are modelled only by simplified outer shapes and homogeneous volumetric source terms for momentum and energy exchange. The prediction of coolant mixing with the new RPV model is improved but the rotation of mixing patterns observed at the core inlet is not correctly reproduced. With the extended loop model a rotation of mixing patterns is predicted but it is significantly overestimated. The consideration of the pump impellers ge-

ometry and a revision of the pump housing geometry seems to be necessary for an improved modelling of swirl of flow patterns. The limitations of the Loop model are given by the computational time, the unavailability of some technical details and by the large development time for a model like this. Therefore the presented results from the Loop model have to be considered as a qualitative study. The experiences assembled in this work will be used for primary loop studies of decay heat removal within the ELSY (European Lead cooled System) project but with less detail resolution.

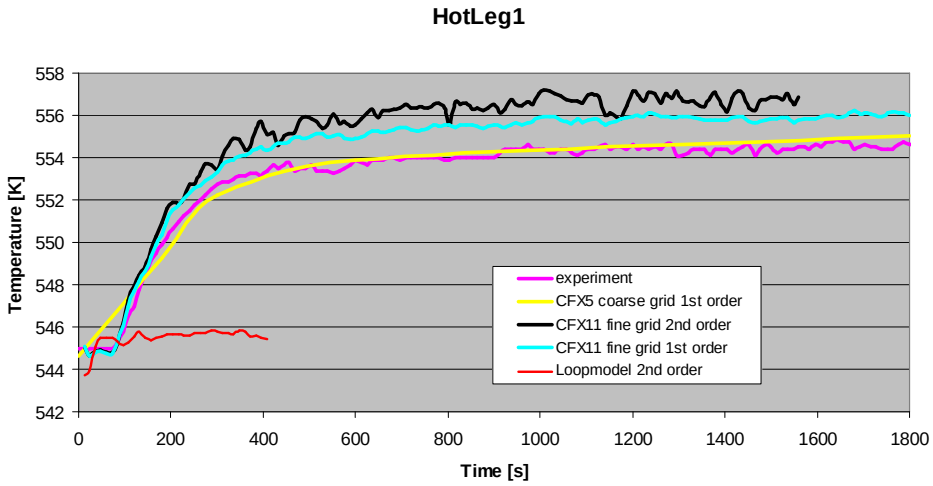

Fig. 13: Temperature at outlet of loop 1

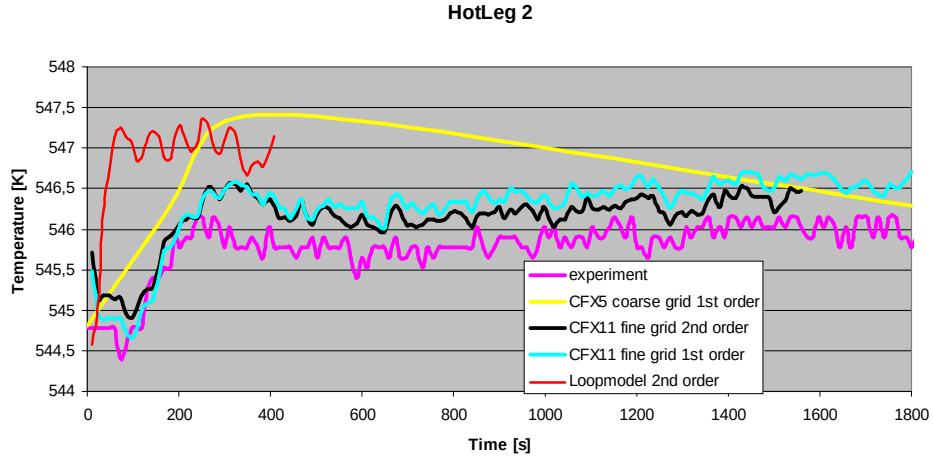

Fig. 14: Temperature at outlet of loop 2

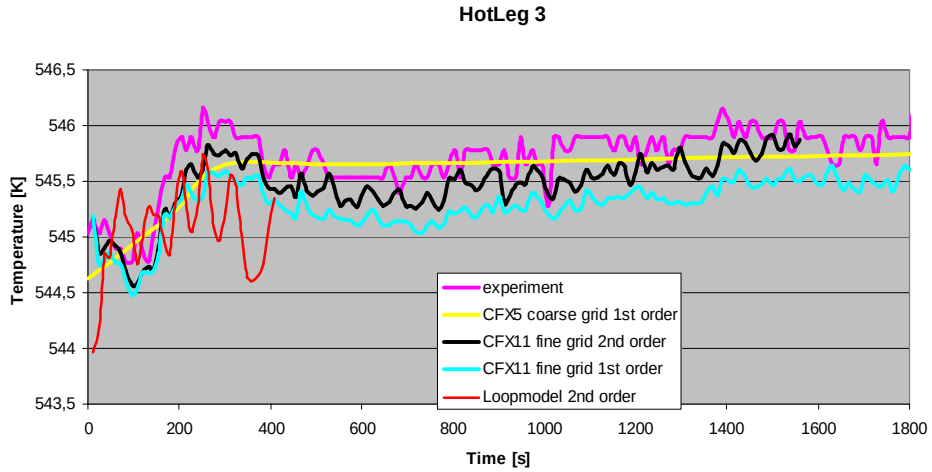

Fig. 15: Temperature at outlet of loop 3

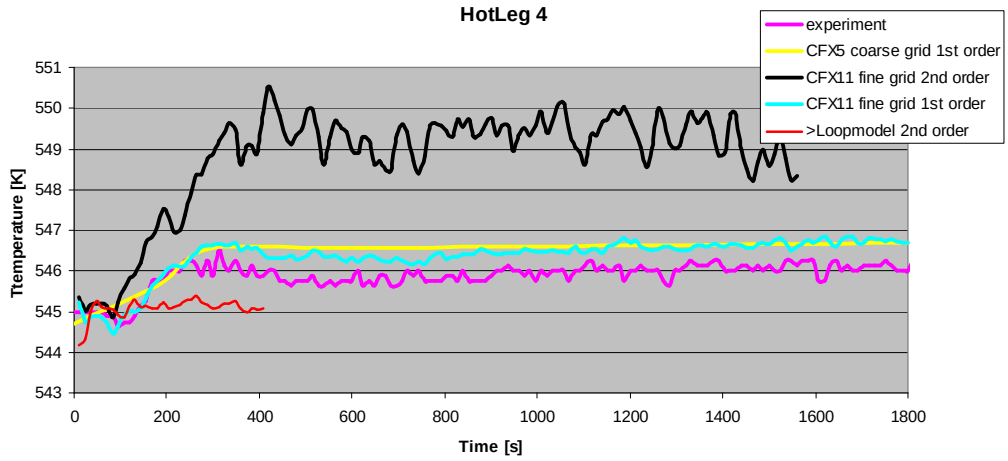

Fig. 16: Temperature at outlet of loop 4

6. References

1. Böttcher, M. (2008). Detailed CFX-5 study of the coolant mixing within the reactor pressure vessel of a VVER-1000 reactor during a non-symmetrical heat-up test. *Nuclear Engineering and Design 238 (2008) 445-452.*
2. Bieder, U., Bétin, S., Fauchet, G., Kolev, N. (2004). Preparation of the thermalhydraulic benchmark V1000CT-2.*OECD/DOE/CEA. VVER-1000 Coolant Transient Benchmark, 2nd Workshop, Sofia Bulgaria.*
3. Kolev, N., Aniel, S., Royer, E., Bieder, U., Popov, D., Topalov, T. (2004). Volume 2: Specifications of the VVER-1000 Vessel Mixing Problems, Commissariat a l'Energie Atomique and OECD Nuclear Energy Agency, *VVER-1000 Coolant Transient Benchmark (V1000CT).*
4. ANSYS CFX, Release 11.0 (2007). *Reference Guide.*
5. Sanchez, V., Böttcher, M. Investigations of the VVER-1000 Coolant transient benchmark phase 1 with the coupled System code RELAP5/PARCS.
6. Programs for the investigation of loop flow mixing in the reactor vessel of Kozloduy Unit 6 (1991). *Kozloduy NPP.*